Netherlands Institute for Space Research

National Institute of Standards and Technology

ATHENA X-ray Integral Field Unit

Microcalorimeter array development for the ATHENA X-ray Integral Field Unit

Presented by Stephen Smith NASA GSFC
On behalf of the X-IFU array development team

Key contributors:
NASA GSFC: J.S Adams, S.R. Bandler, J.A. Chervenak, A.M. Datesman, M.E. Eckart, A.J. Ewin, F.M. Finkbeiner, R. Hummatov, R.L. Kelley, C.A. Kilbourne, A.R. Miniussi, F.S. Porter, J.S. Sadleir, K. Sakai, N. Wakeham, E.J. Wassell
SRON: H. Akamatsu, L. Gottardi, R.H. den Hartog, B.D. Jackson, J. van der Kuur.
NIST: D.A. Bennett, W.R. Doriese, G.C. Hilton, D. Swetz, J.N. Ullom.

Athena X-IFU Baseline Array Configuration

- Currently assumed X-IFU baseline
  - Uniform *Large Pixel Array - LPA*.
  - 3840 identical transition-edge sensor (TES) pixels, 0.25mm pitch.
  - ΔE_{FWHM} = 2.5 eV @ 7 keV.
  - Baseline changed in Nov 2016 to make use of defocusing optic (for high rate point source observations).
  - Reduces count-rate requirement to ~ few cps, enables reduced speed pixels (~x2-3) and more optimal use of available readout resources (greater engineering margin).
    - **LPA-1 -> LPA-2**

Large pixel array (LPA)

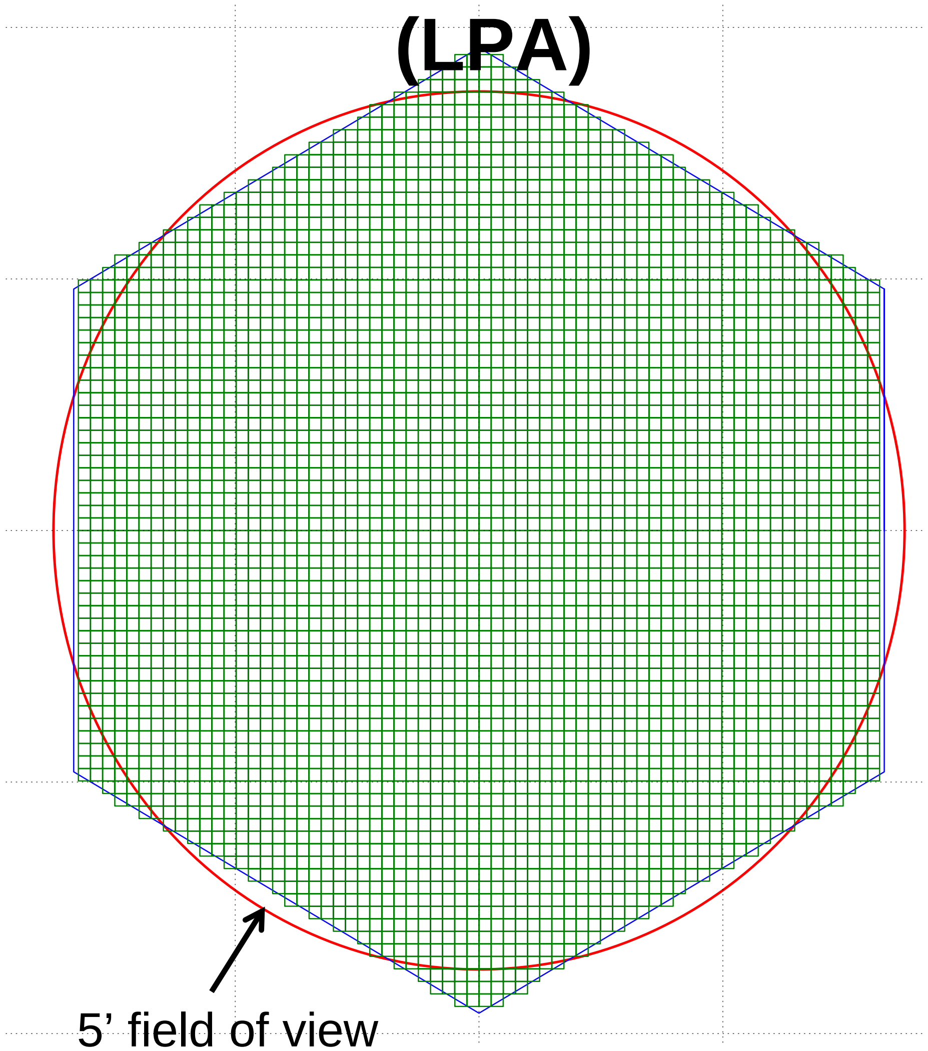

Transition-edge sensor arrays, 2016 state of the art

ATHENA X-ray Integral Field Unit

- Previously proposed “LPA-1” GSFC TES pixel.
  - Mo/Au Bilayer TES, target T_C ~ 90 mK, suspended on SiN (~ 1 μm).
  - Low impedance TES, R_n = 10 mΩ.
  - Composite Au/Bi electroplated absorbers (low heat-capacity and fast thermalization).
  - Thermal conductance G_b = 200 pW/K, Fast ~ 400 μs decay times (originally for LPA-1, 10’s cps / pixel).

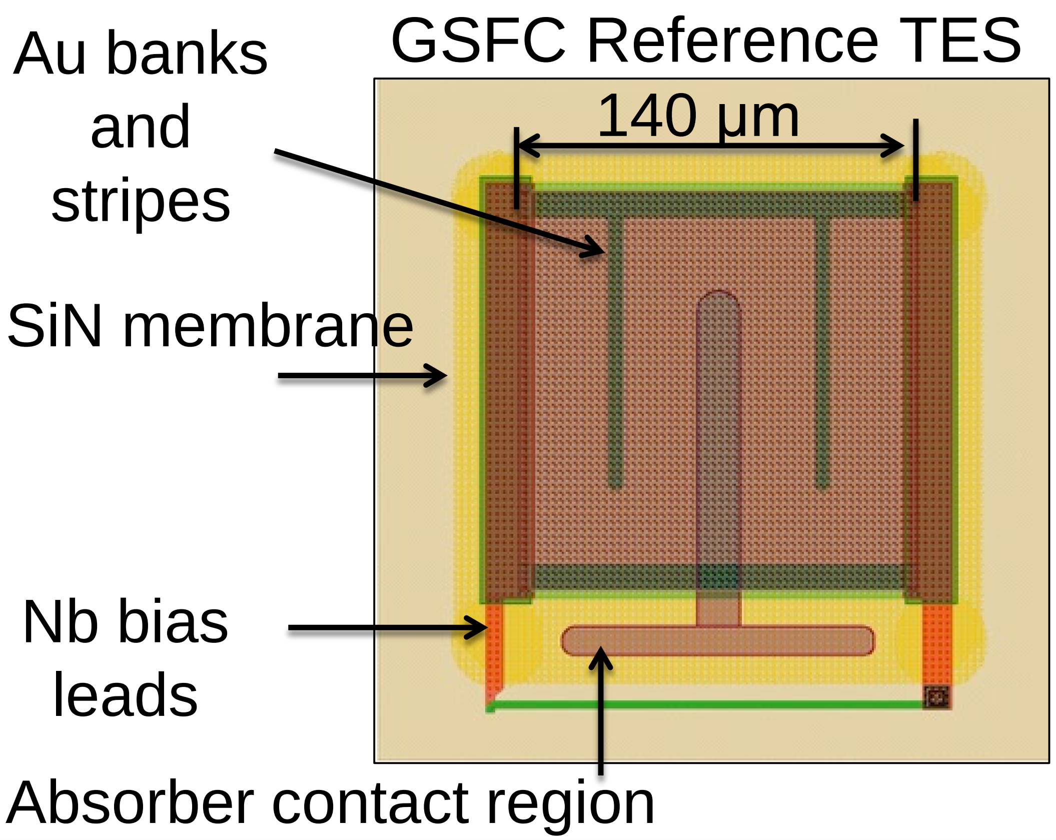

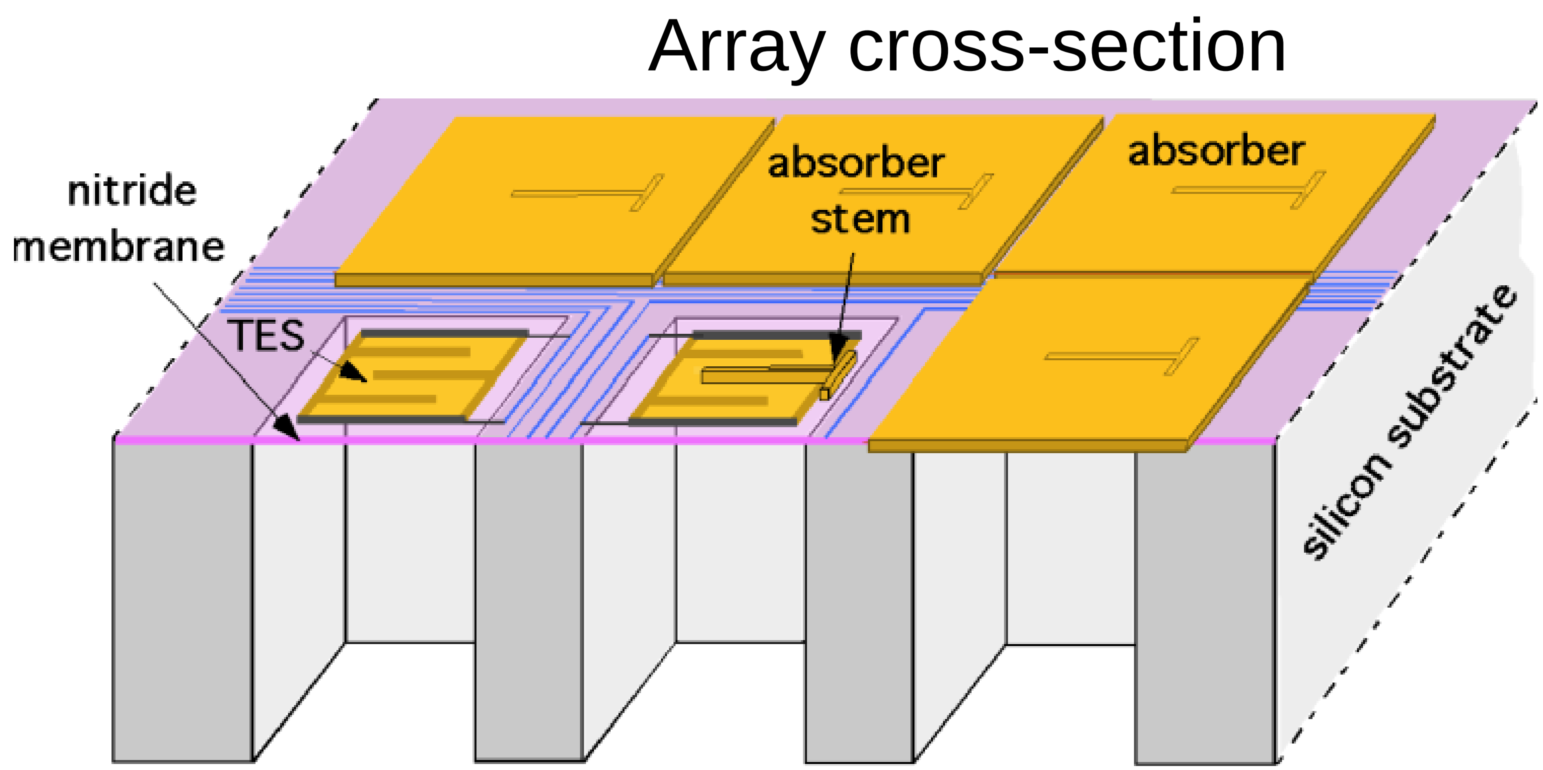

Transition-edge sensor arrays, 2016 state of the art

- GSFC devices were historically optimized for ***Time Division Multiplexing* (TDM)** approach under study as back-up.
  - See J. Ullom et al. 10699-60 @ 4:30pm
- However baseline readout approach uses ***Frequency Division Multiplexing* (FDM)**.
  - See H. Akamatsu et al. 10699-58 @ 4:00pm

- In TDM TESs are DC biased (multiplexing via switching SQUIDs).
  - TES transition is independent of the muxing.
- In FDM the mux encoding via AC TES bias with different frequencies.
  - In Mo/Au TESs lead to frequency dependent variations in TES transition shape and degraded resolution performance.

Pixel optimization activities

- Technology development focused on 3 main areas:

  (1) Pivot towards lower count-rate 'LPA-2'.

  - x2-4 slower pixels, control of thermal conductance to the heat-sink via TES size / membrane thickness.

  (2) Uniformity optimizations.

  - Exploring better transition uniformity, less sensitive to environment (role of stripes, size effects).

  (3) Reduce the impact of frequency dependent effects in the AC-TES.

Mixed arrays for transition and G_b studies

- Pixel size. G_b scales with TES phonon emitting perimeter.

140 -> 50 μm => 3x reduction in G_b.

- Impact of geometry (pixel size/metal features) on transition shape.

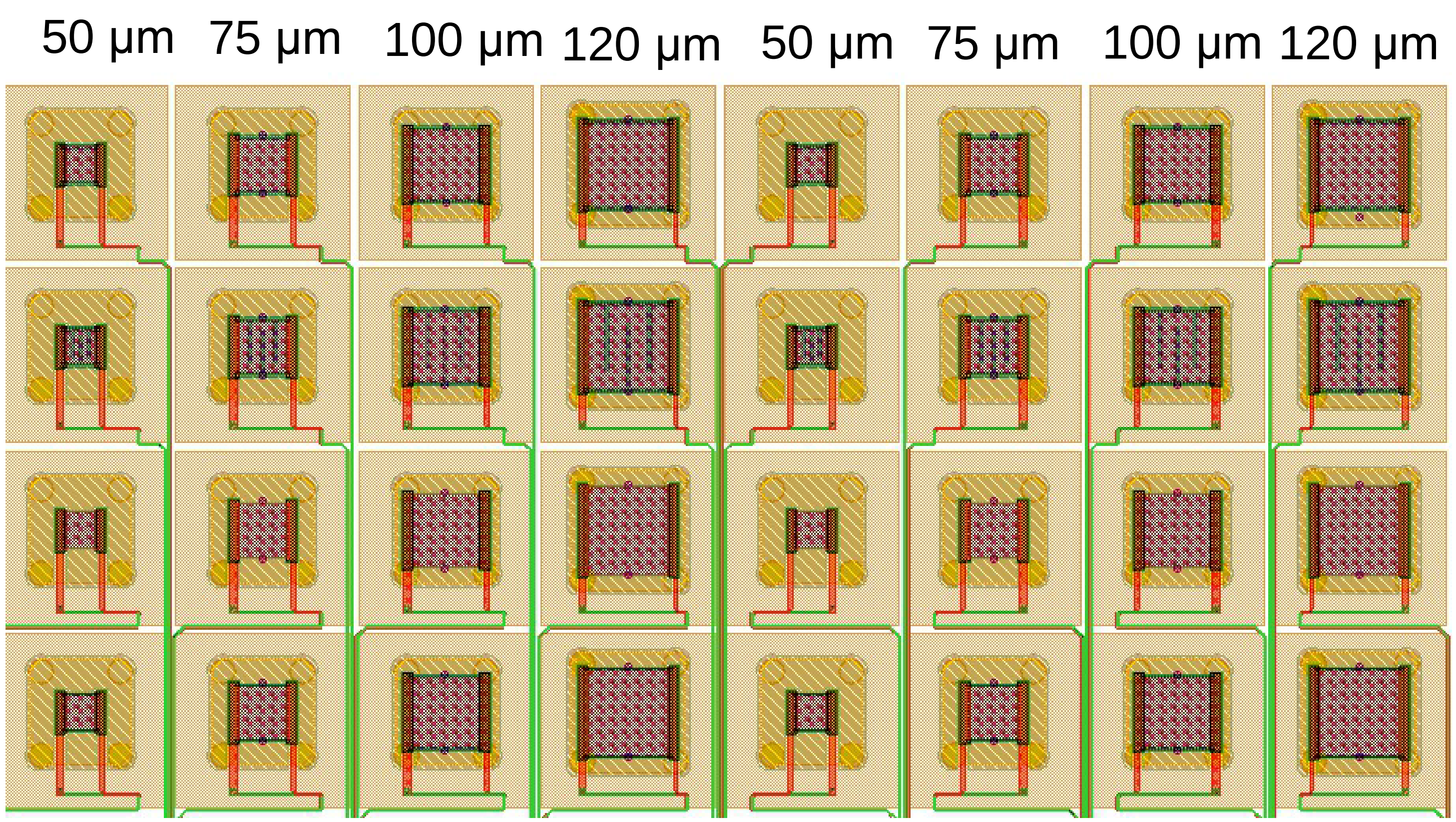

DC transition studies – studying role of stripes

- LPA optimization activities has led to growing understand of geometry effects in TESs.
  - Exploring the role of stripes, historically used on larger TESs for noise and transition shape control (empirically).
  - Measurements in large arrays show undesirable variations in transition shape.
    - Presence of 'kinks' hard to predict and can impact array uniformity.
    - Improving understand of how they come about / evolve – See Wakeham et al., LTD-17, 2017.
    - Maybe due to alignment difference between the different metal layers (stripes/stems).

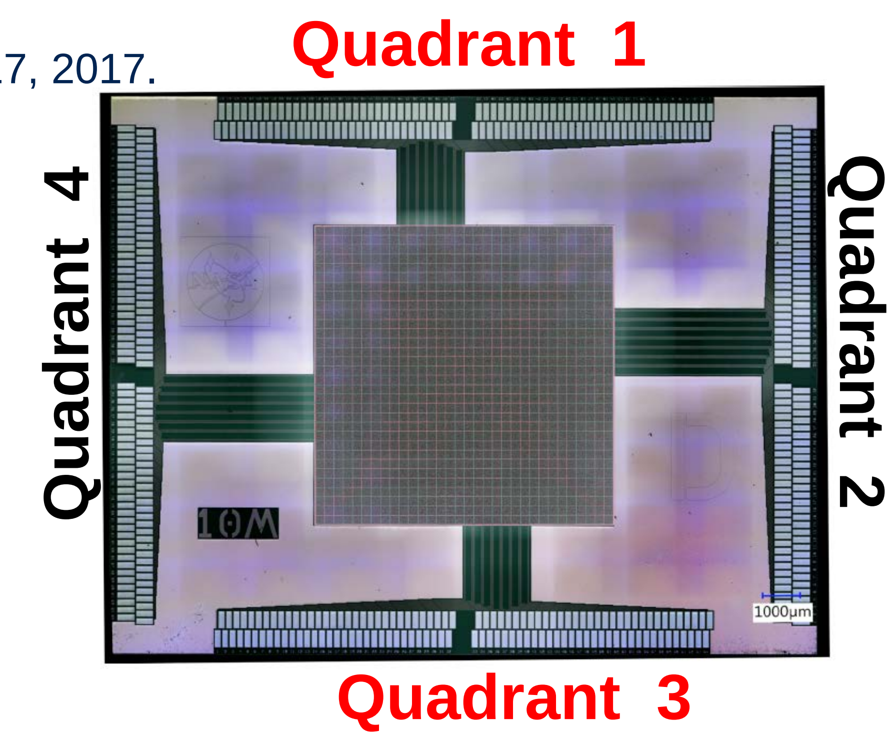

<u>Different transition shapes in different quadrants of 32x32 array</u>

Q1 and Q3 have majority 'kinked' transition

Q2 and Q4 had majority 'smooth' transition

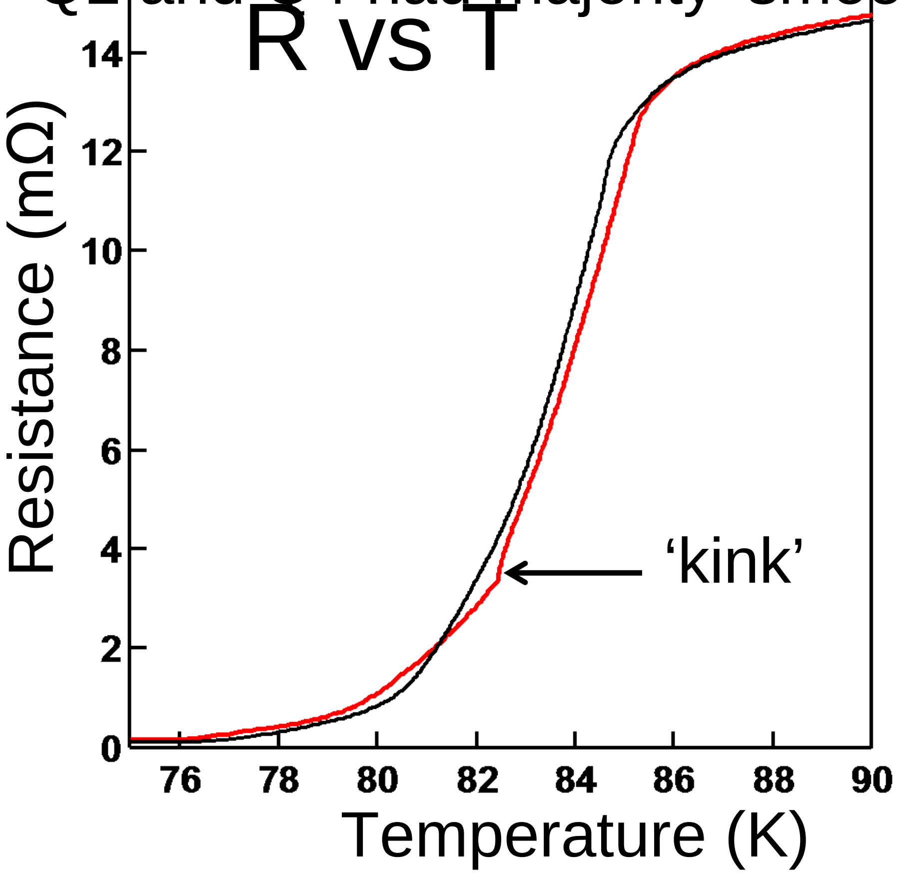

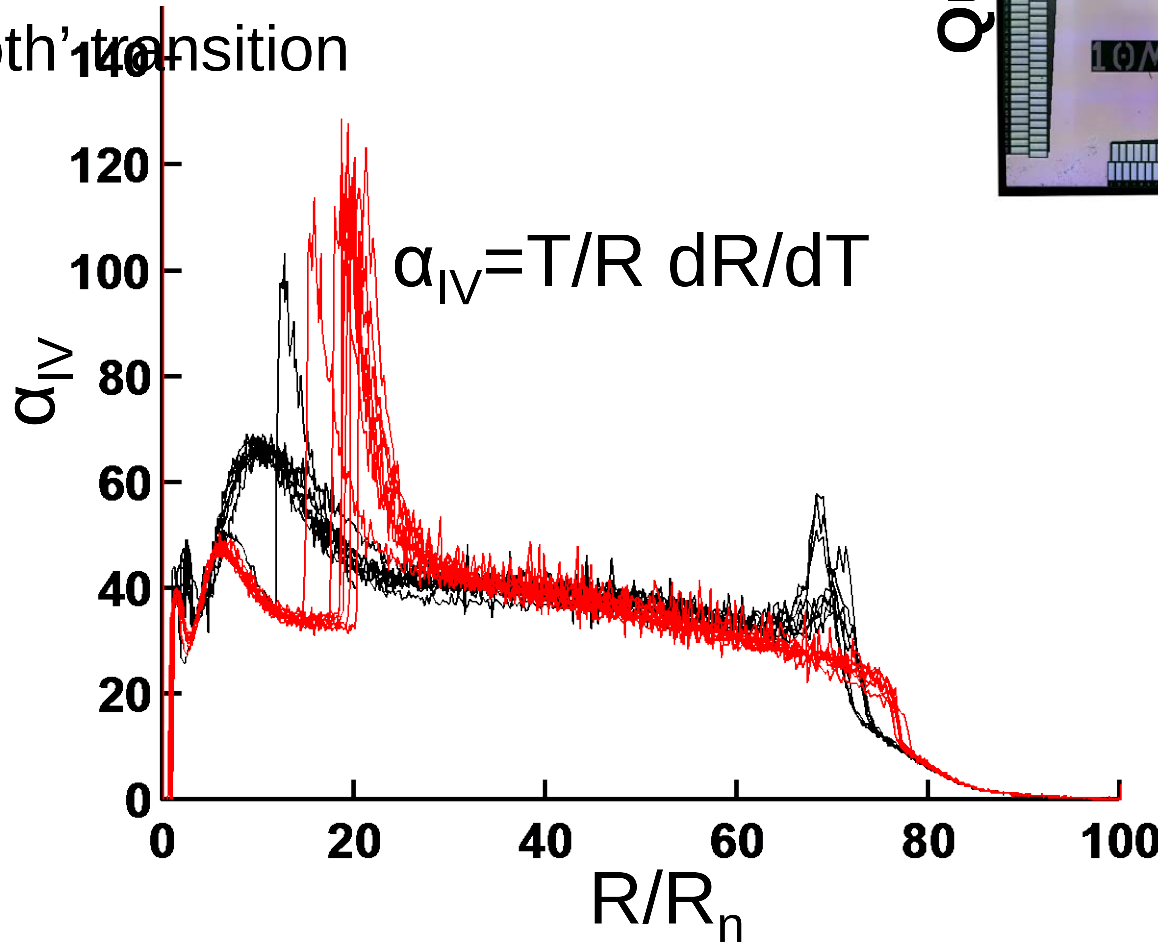

2 Stripes + T-stem

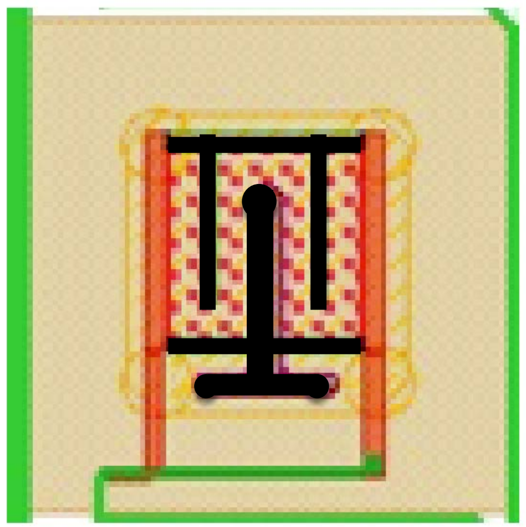

DC transition studies – studying role of stripes

- LPA optimization activities has led to growing understand of geometry effects in TESs.
  - Exploring the role of stripes, historically used on larger TESs for noise and transition shape control (empirically).
  - Measurements in large arrays show undesirable variations in transition shape.
    - Presence of 'kinks' hard to predict and can impact array uniformity.
    - Improving understand of how they come about / evolve – See Wakeham et al., LTD-17, 2017.
    - Maybe due to alignment difference between the different metal layers (stripes/stems).

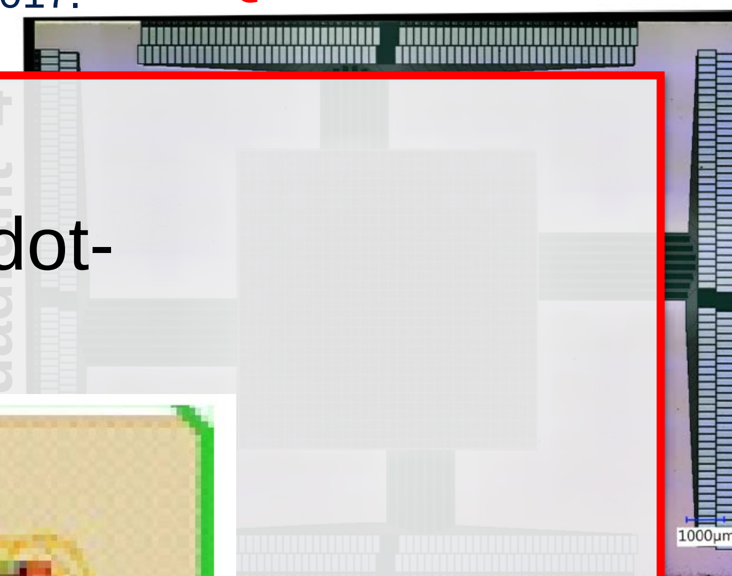

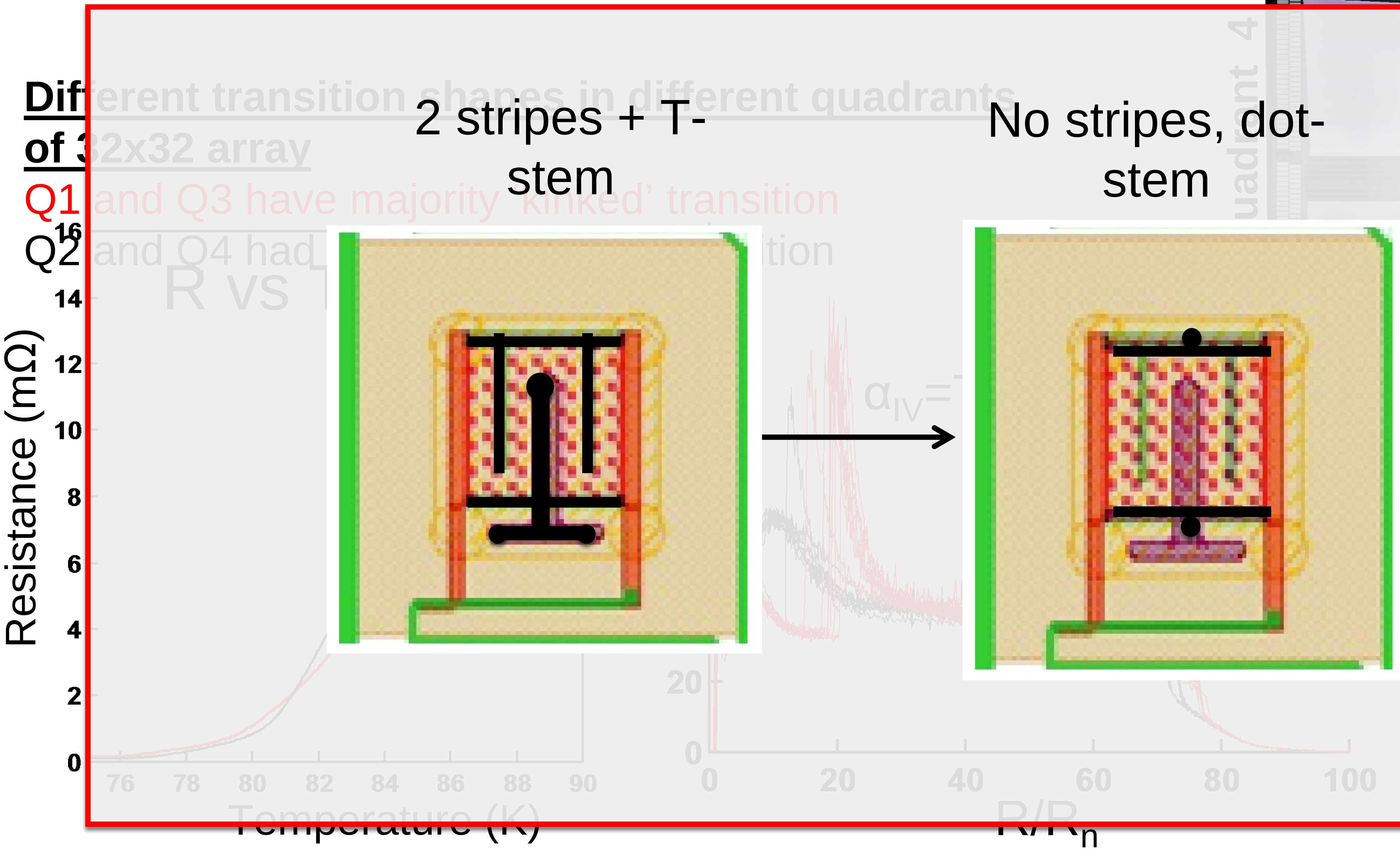

First uniform kilo-pixel arrays of no-stripe pixels

- First uniform 32x32 arrays, no stripes, 50/75/100/120 µm, 250 µm pitch.
- Example for 50 µm devices, show good DC transition shape and uniformity.
- Large transition phase space with no kinks, less sensitive to environment (B-field)

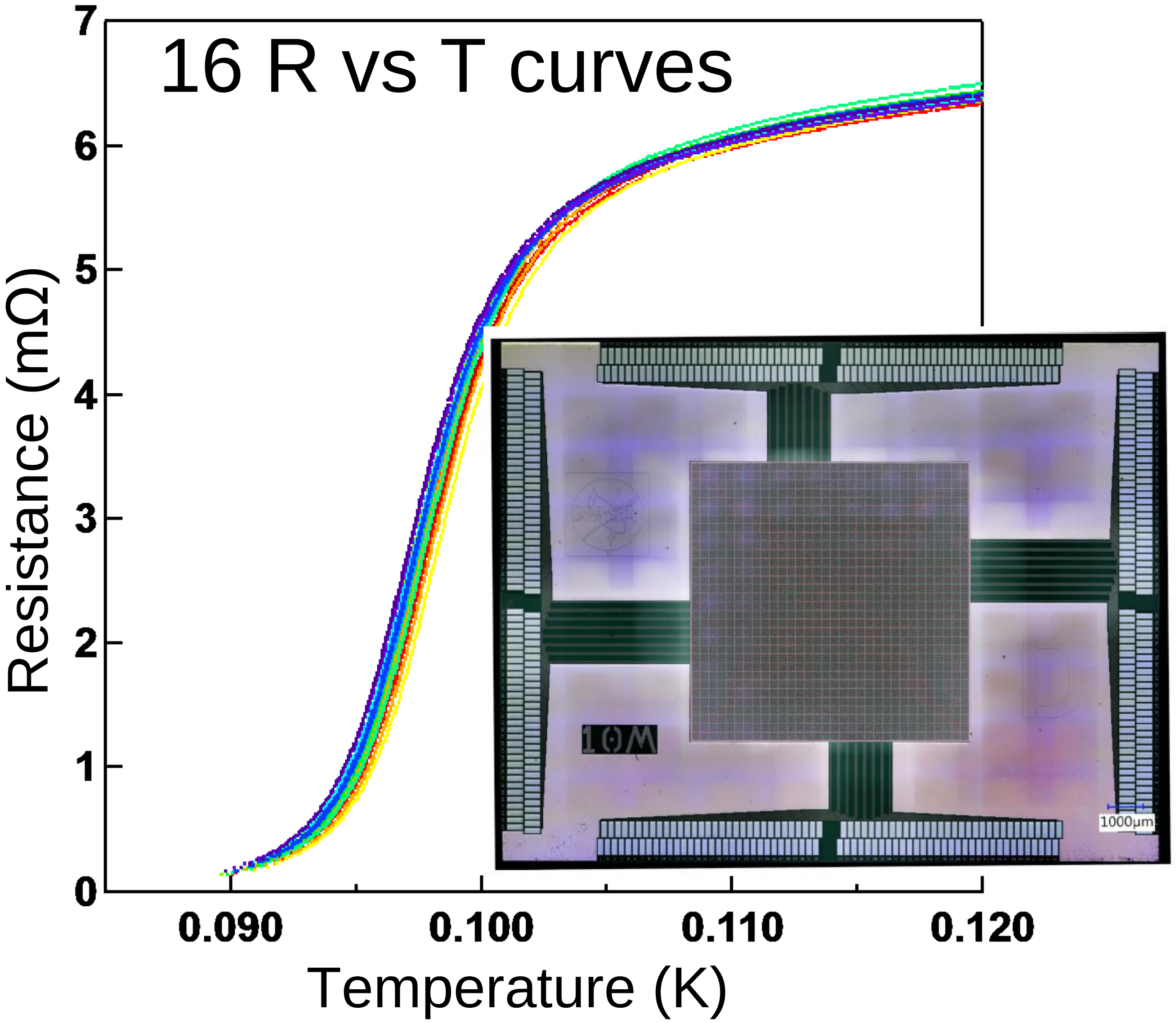

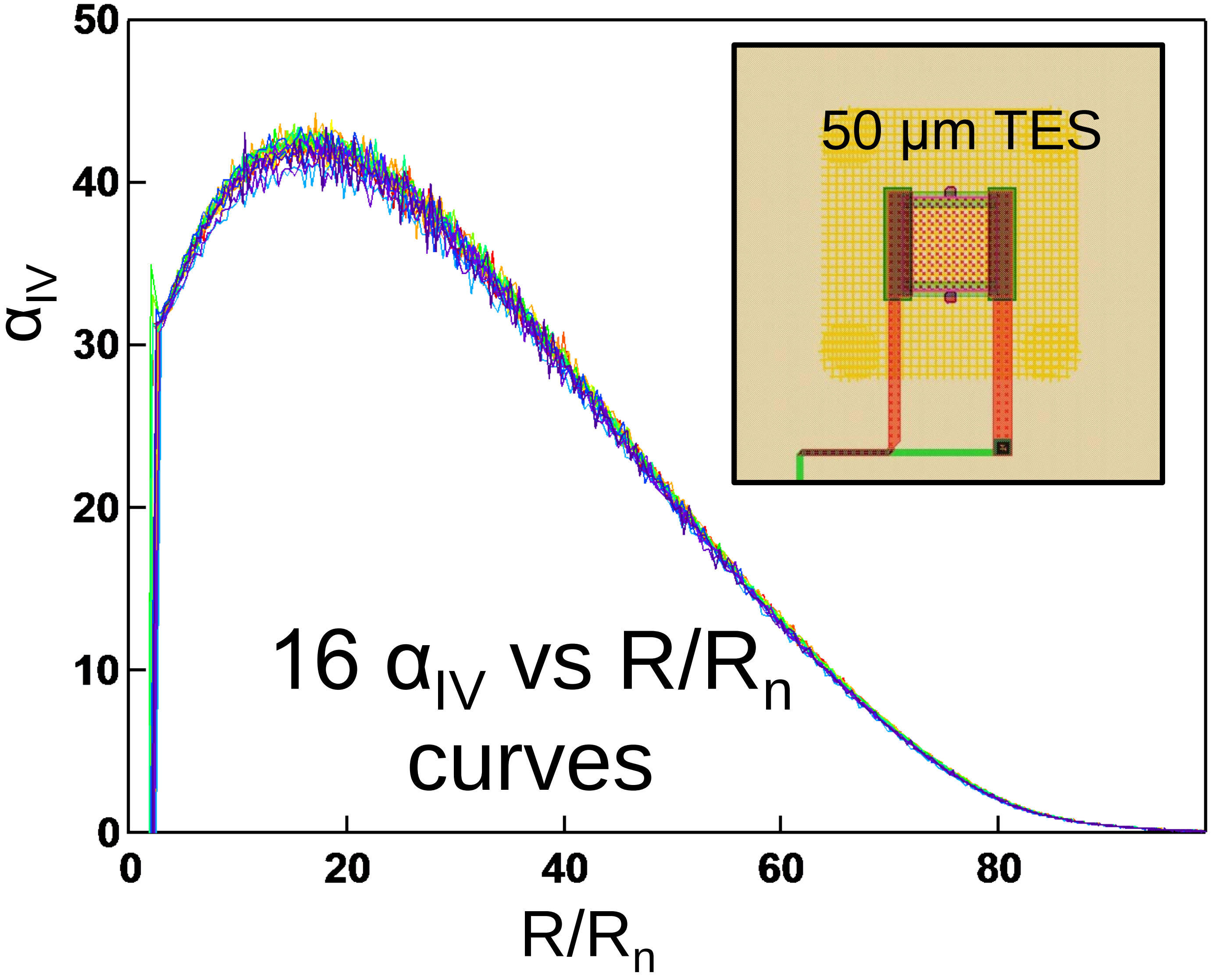

DC transition studies – example 50 μm TES, no stripes

- Good pulse shape and noise uniformity.
- DC performance is excellent, ΔE_{FWHM} consistently at 2.0 eV level.
- Smaller TES sizes. G_b = 75 pW/K at T_C = 90 mK.
  => slower speed τ = 2.2 ms.

Very promising LPA2 DC pixel understudy for use with backup TDM readout.

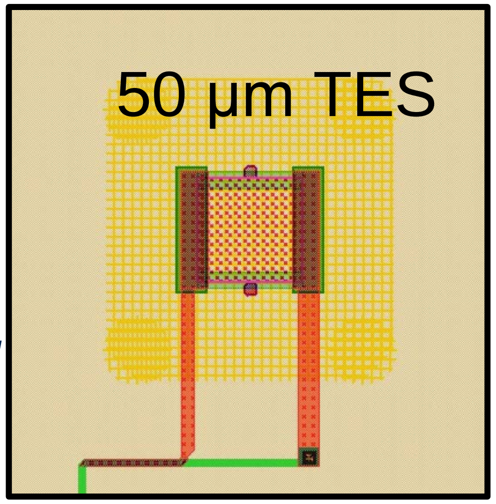

Average pulse shapes for10 pixels at 15% R_n

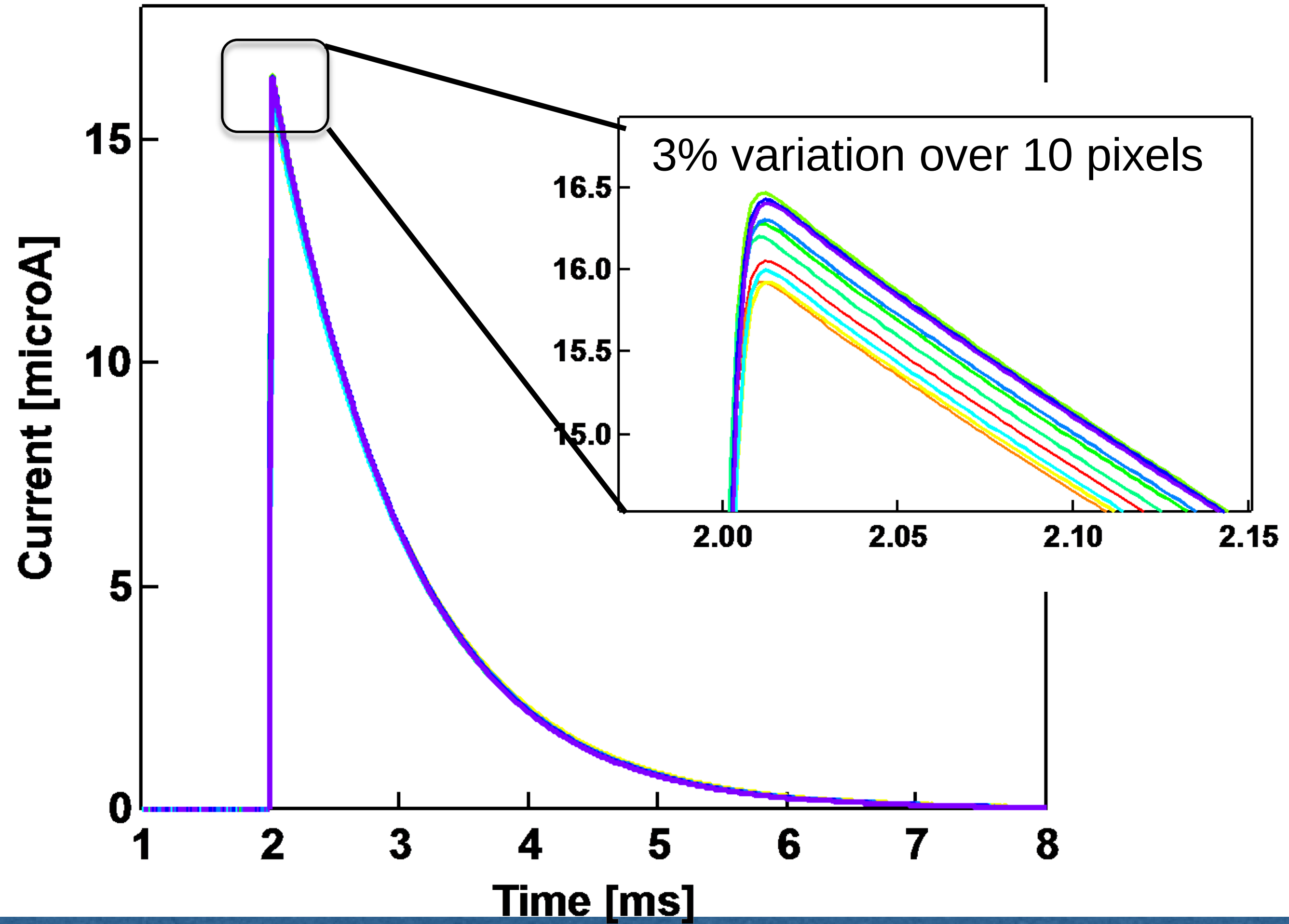

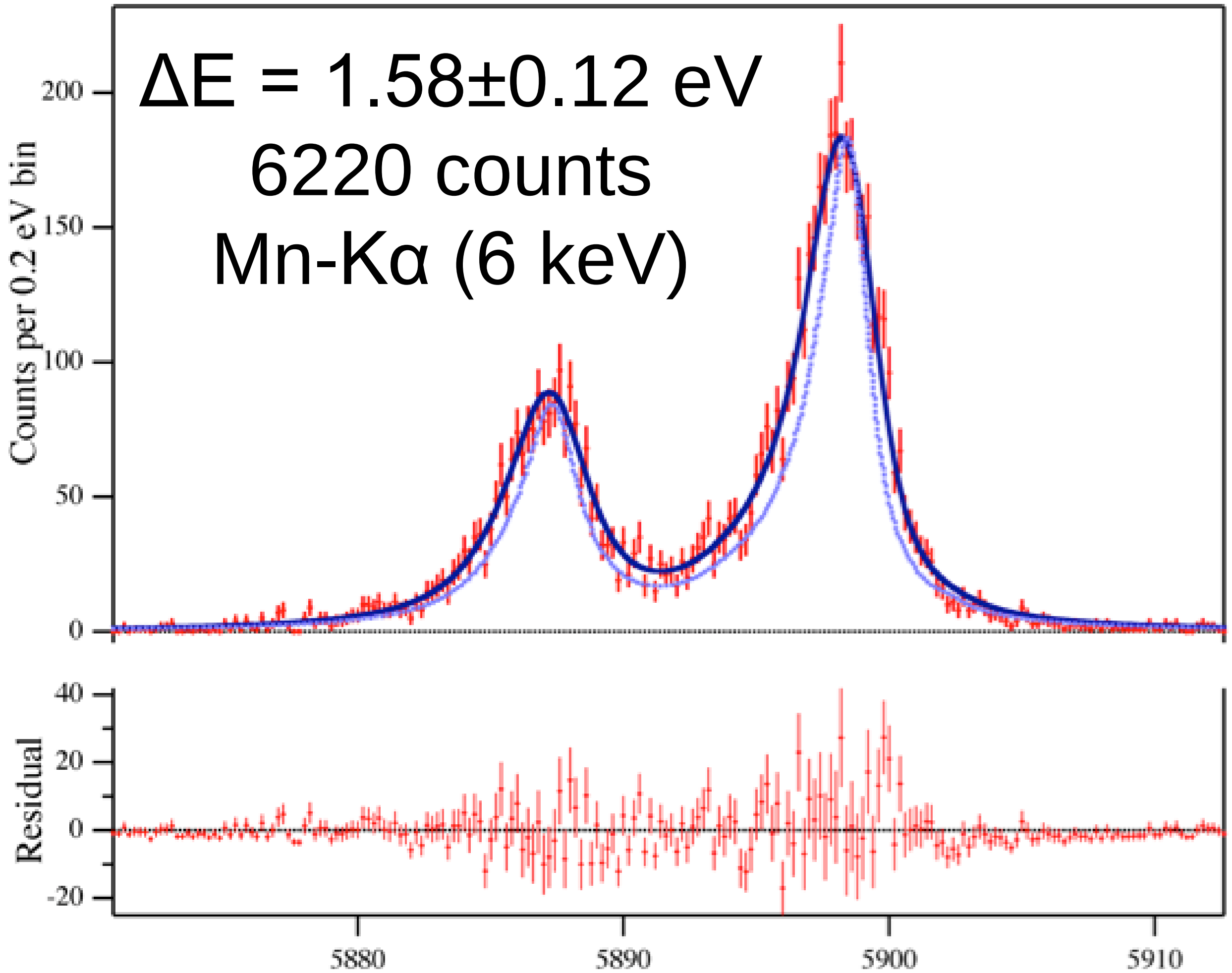

Miniussi et al. 2017

AC Pixel optimization activities

ATHENA X-ray Integral Field Unit

- Large collaborative effort NASA/SRON/NIST to understand frequency effects in AC TES.
- Identified two main contributors:

1) AC, dissipative, losses (magnetic coupling to nearby metals) broadens transition (lower α). Limits access to most sensitive part of the transition used to achieve < 2.5 eV. [Sakai et al 2017].

2) **AC Josephson reactance**, periodic steps through the transition due to variation in Josephson inductance. Undesirable non-linearity and noise properties, hard to find good bias points. [Gottardi et al 2017].

Example R vs T 50 µm TES

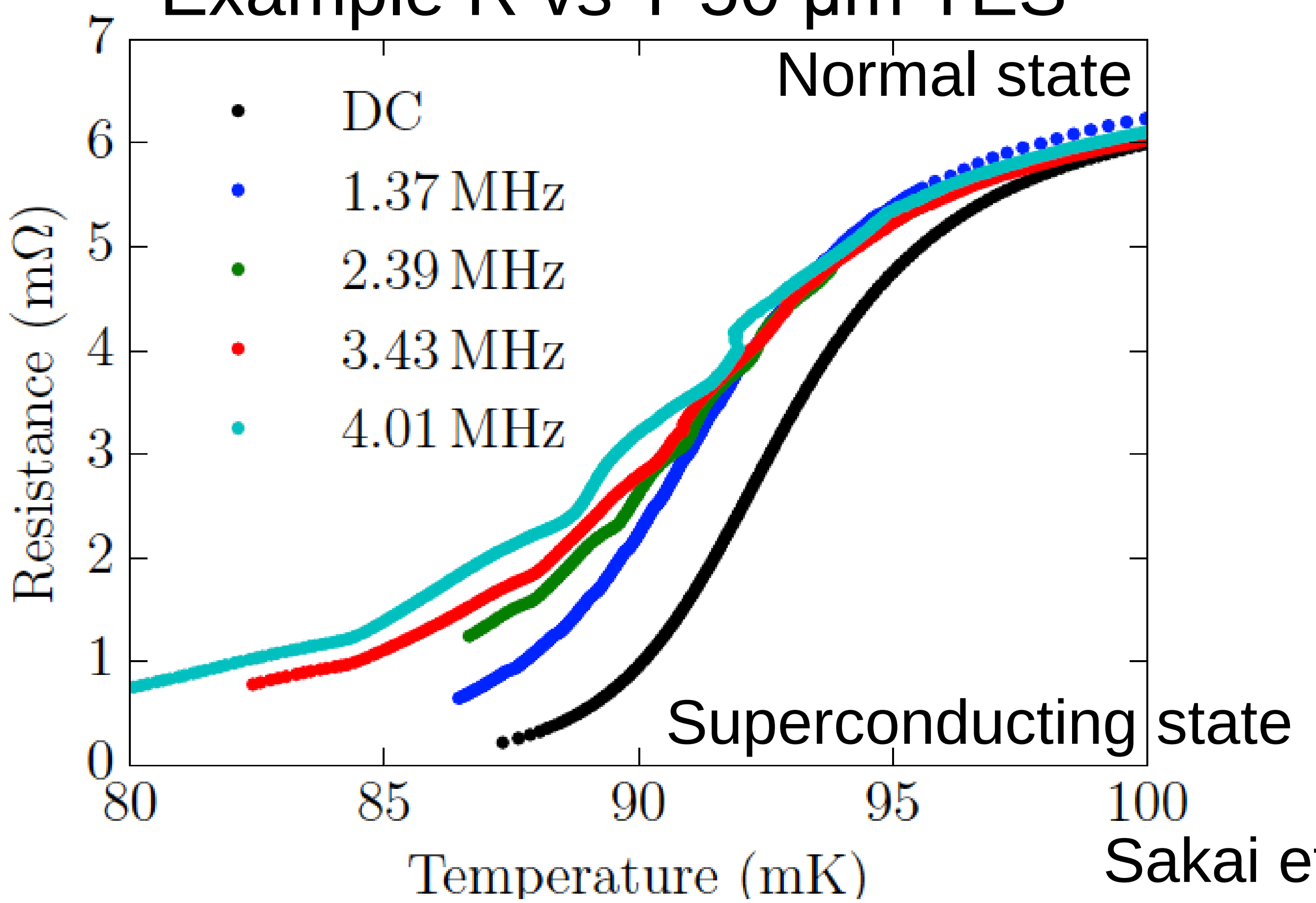

α_{IV} vs R/R_n

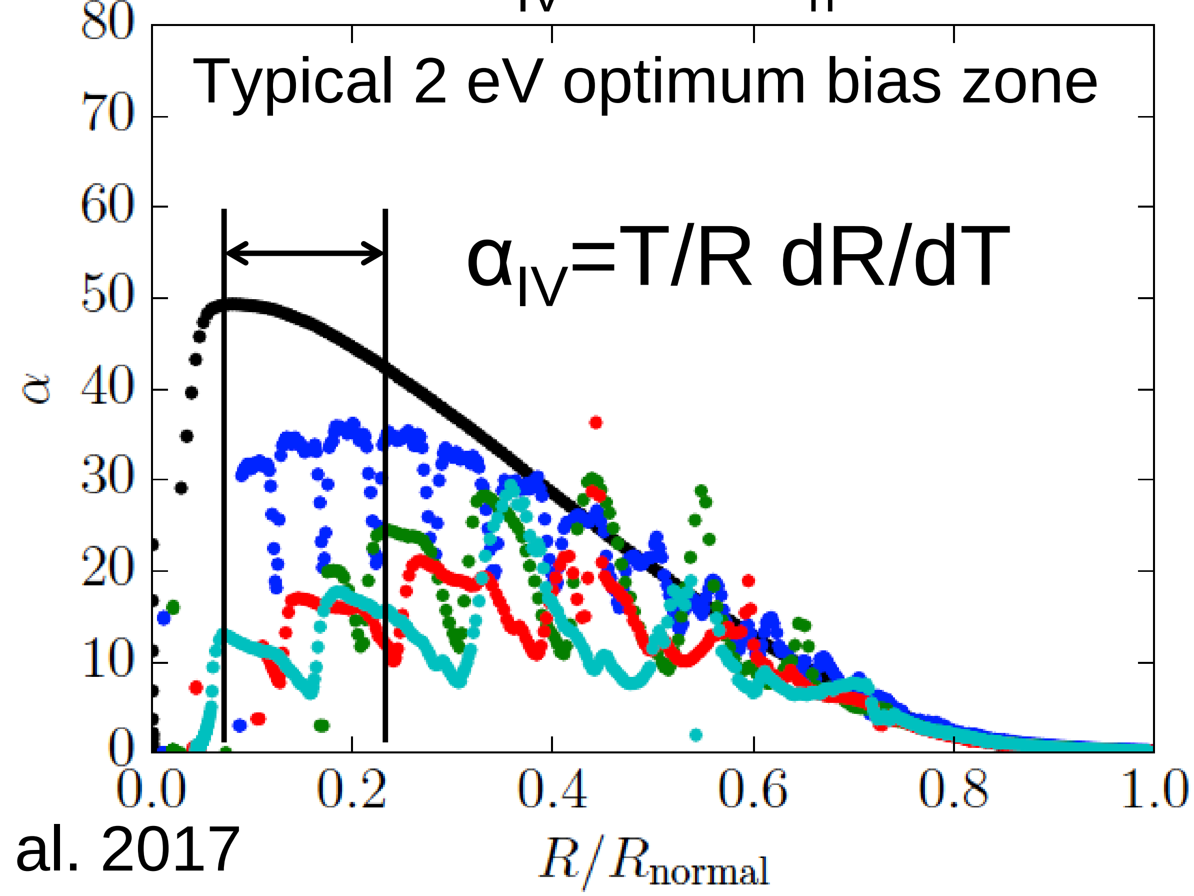

Sakai et al. 2017

AC loss and Josephson-effect mitigation strategies

- Comparison of many different geometries and improved theoretical understanding has led to optimization routes.
- Strategy is to explore higher resistance regime in GSFC Mo/Au TES.
  - AC loss independent of TES Z => higher Z bias point reduces impact of fixed AC loss.
  - High Z devices have small Josephson oscillations.
    - Seen for example in SRON Ti/Au very high-Z devices 200 mΩ [P. Khosropanah, 10699-57]
  - Challenge is to increase Z enough, without affecting other noise or uniformity properties.

1) 15 -> 50 mΩ/□ bilayer sheet resistance. Thinner TES films. Now implemented and in testing.

2) Change aspect ratio (1:1 -> 1:0.25). Longer and thinner. Now implemented and in testing.

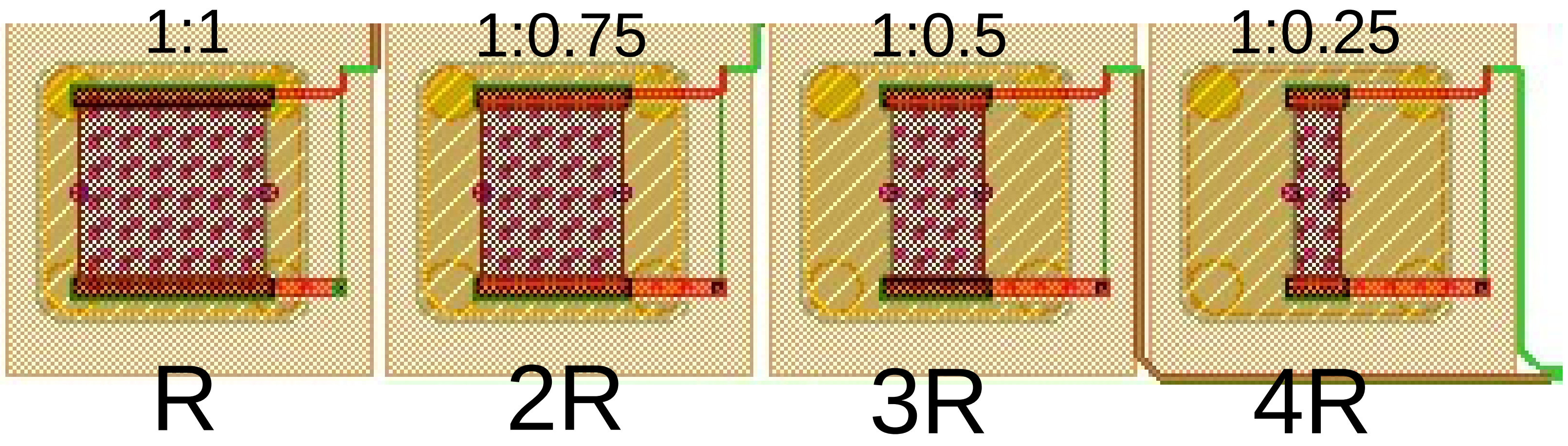

First high-Z devices with good DC performance

DC measurement of 120 μm TES
R_n = 32.7 mΩ (increased from 9 mΩ)

- No additional thermal noise.
- Same achieved ΔE as low-Z films
- Larger TES => steeper transition
- C = 1.5 pJ/K, Au 2.30 μm / Bi 3.39 μm
  – increased x2 to maintain linearity

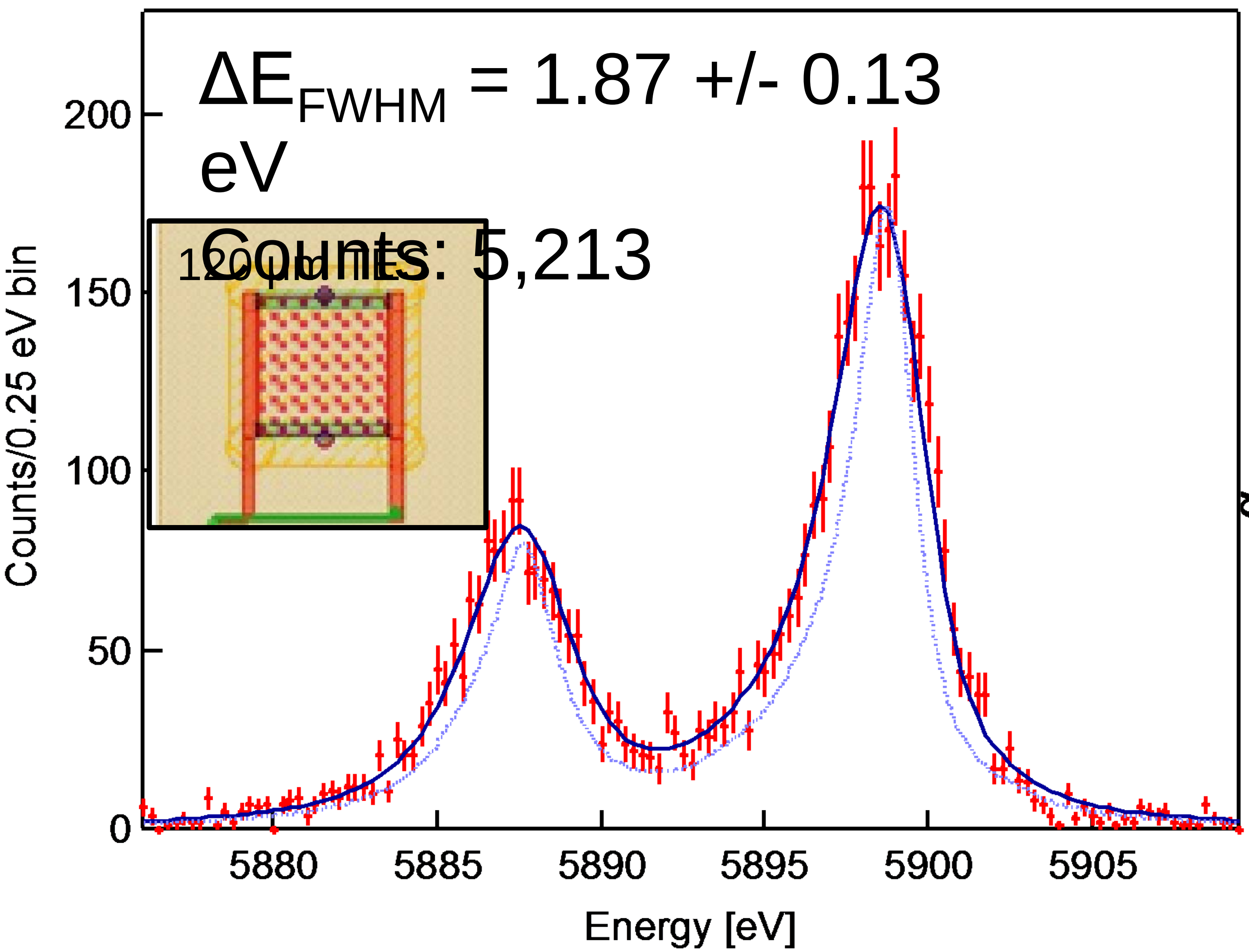

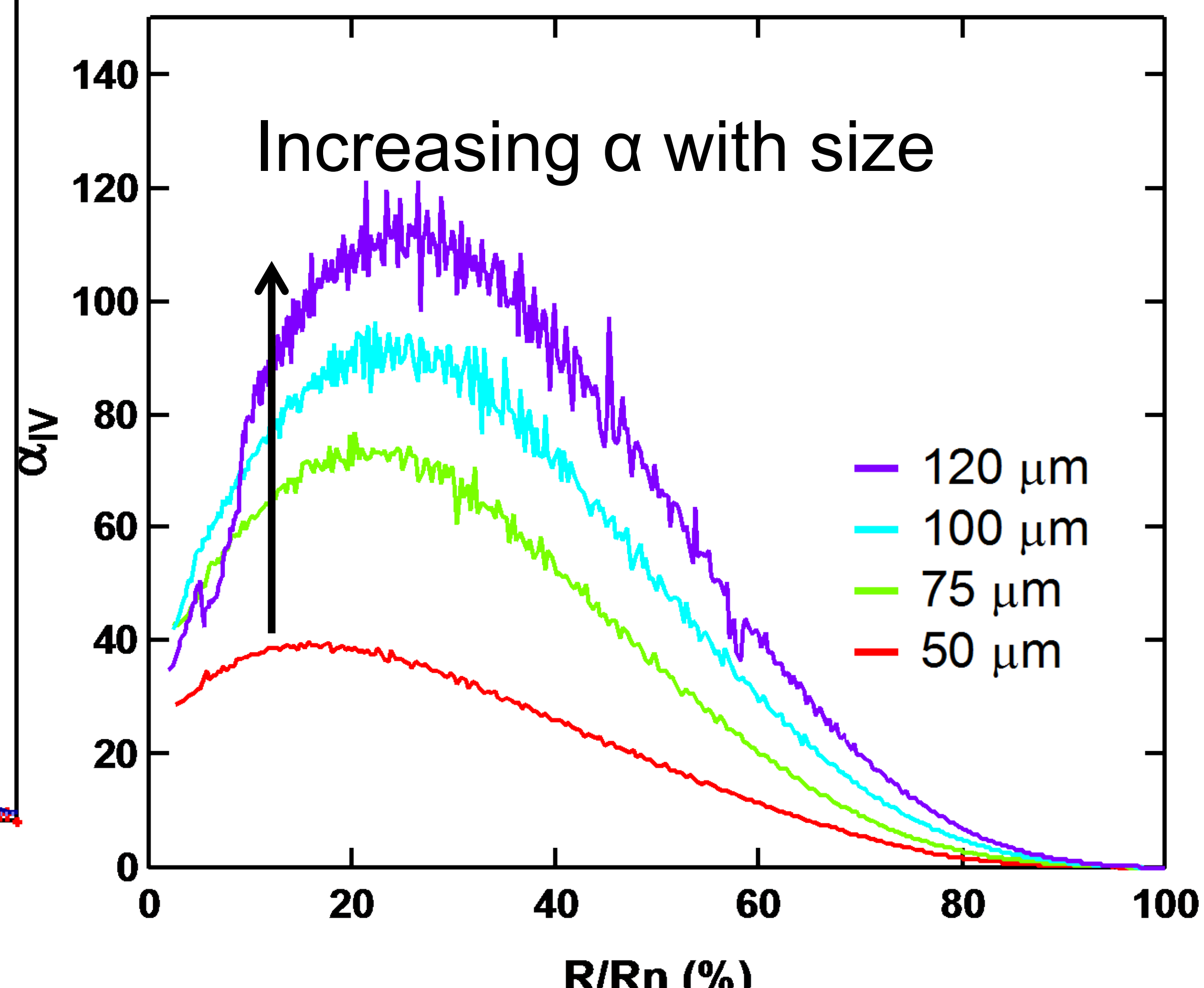

First results on high-Z TES under AC bias at SRON

- *First spectral measurements on mixed arrays at SRON yielded AC-TES x-ray resolution comparable to DC.*
- Best performance seen in 100/120 µm sizes. Smaller, slower 50 µm sizes not as good performance.
- Less structure + more access to lower bias points. => consistent access to < 2.5 eV 1-5 MHz range.
- Later presentation by H. Akamatsu will show more results and FDM testing from 1-5 MHz

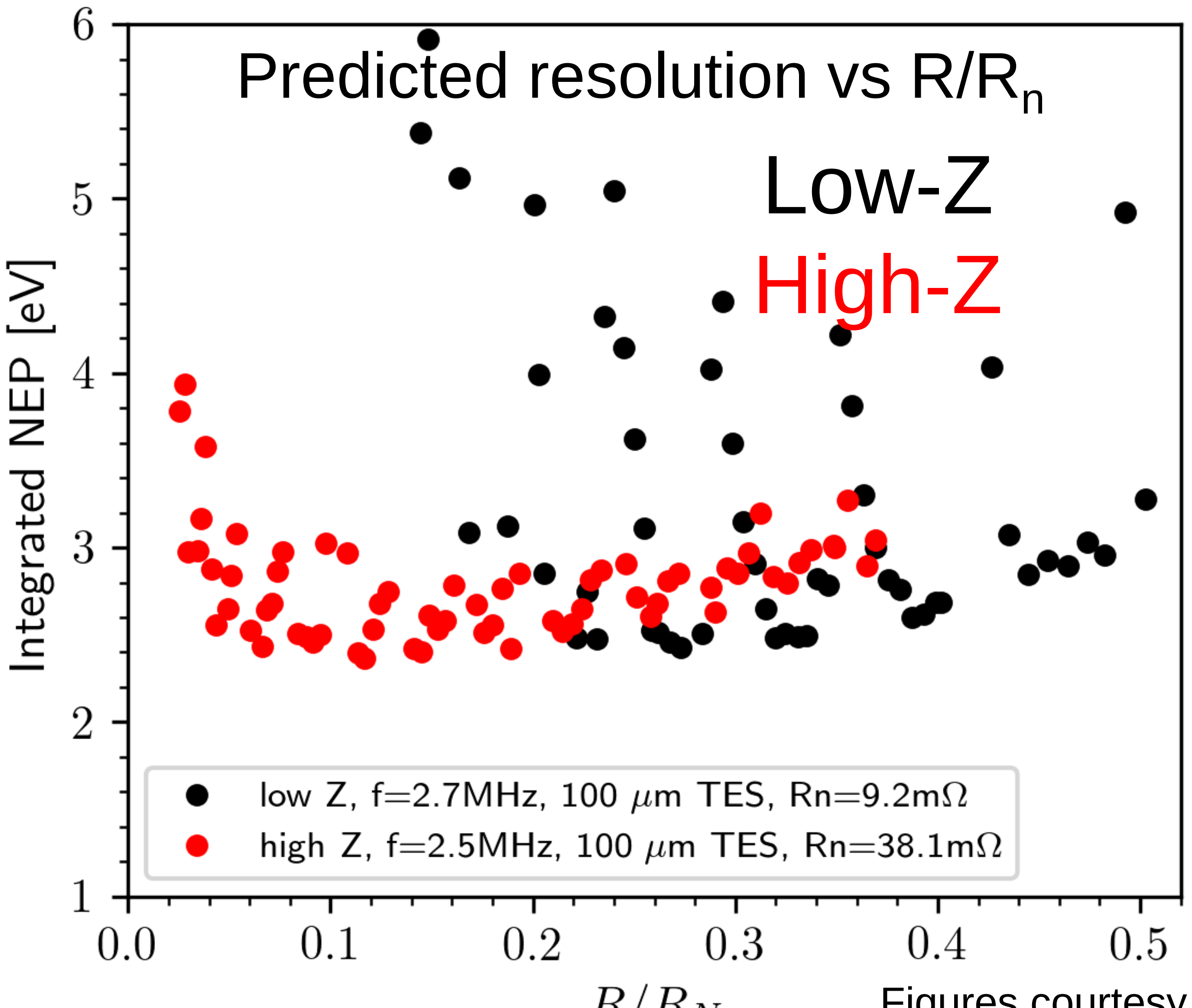

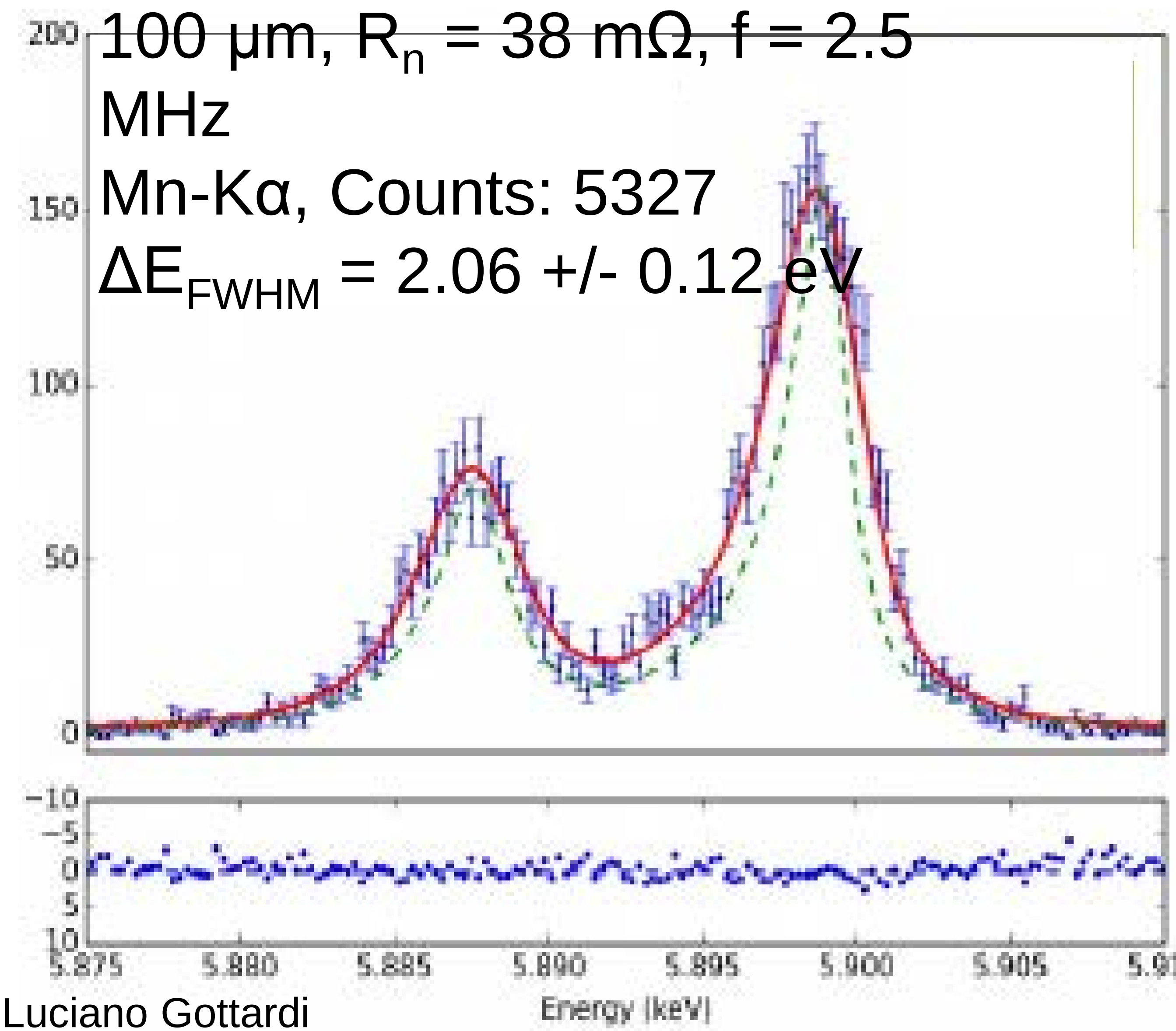

Figures courtesy Luciano Gottardi

First uniform high-Z arrays suitable for large scale FDM demonstrations

- Two 32x32 arrays screened at GSFC and sent to SRON for 40-pixel FDM testing.
- Good DC transition properties and uniformity, R vs T, pulse shape, ΔE.
- $\langle \Delta E_{FWHM} \rangle$ = 1.95 eV for 6 pixels tested.
- Larger TES size => Pixels are fast => for X-IFU may still need to slow these down.

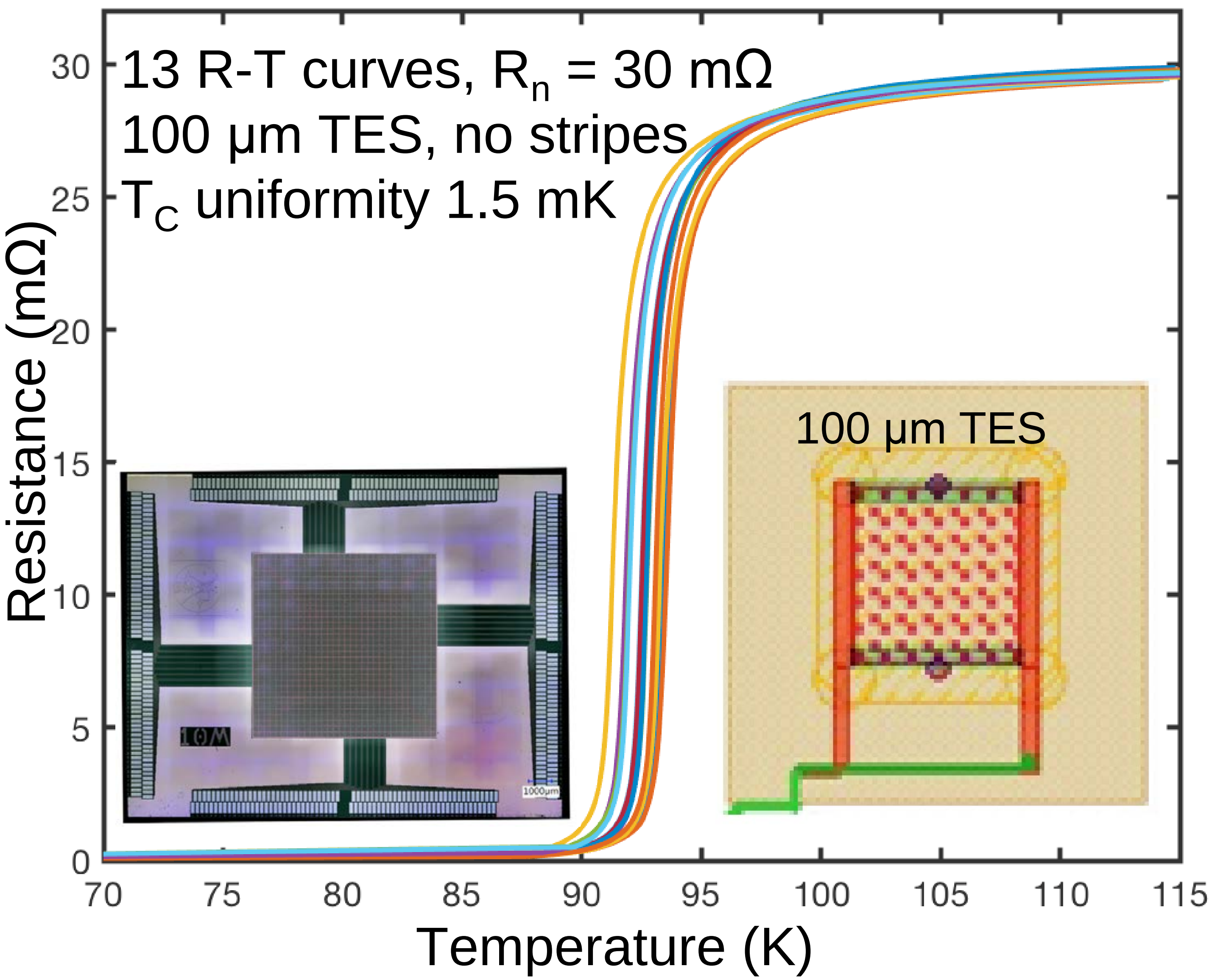

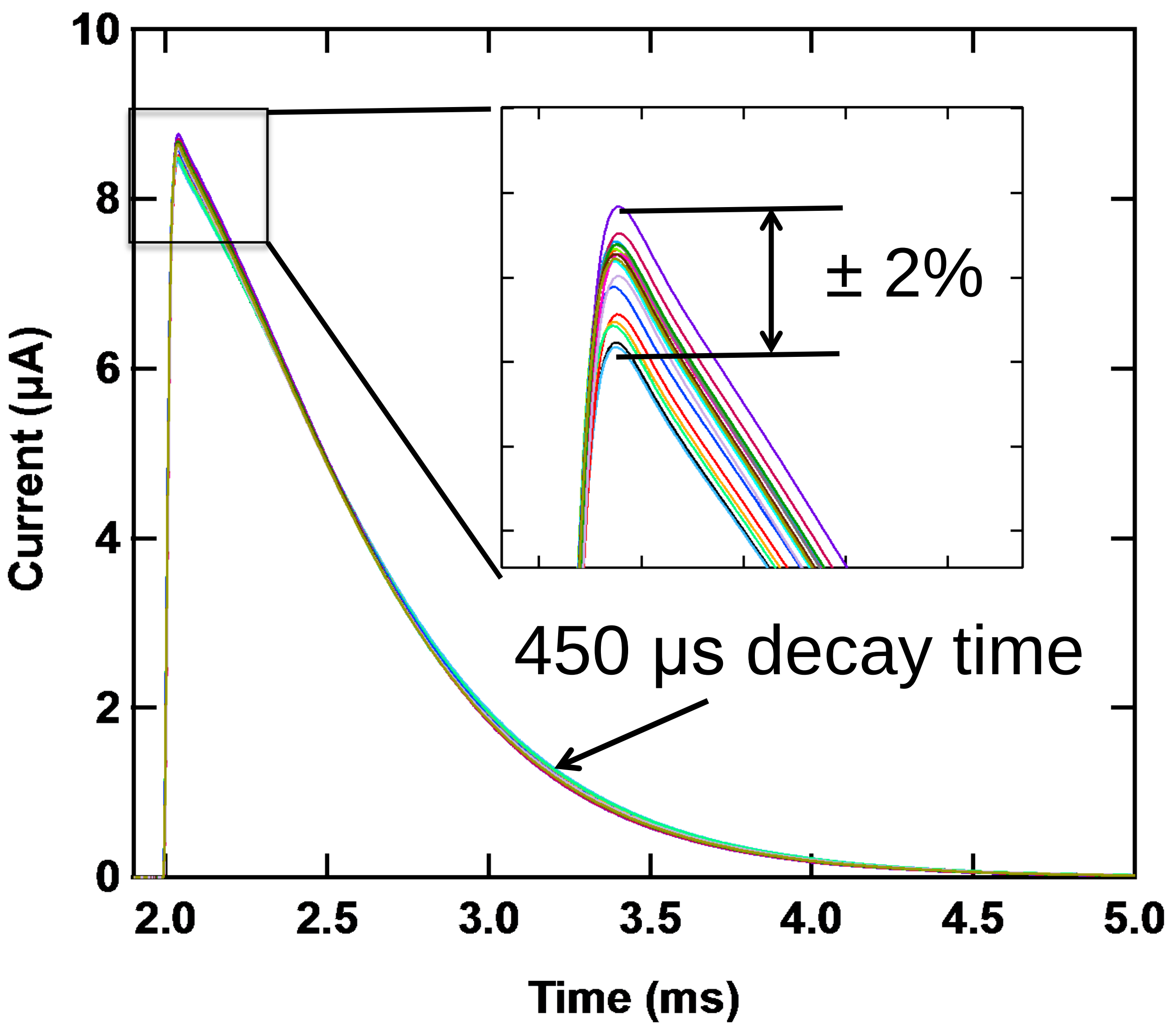

First DC results from high aspect ratio 120 μm TESs

1:0.75

R_n = 54 mΩ, G_b = 113 pW/K

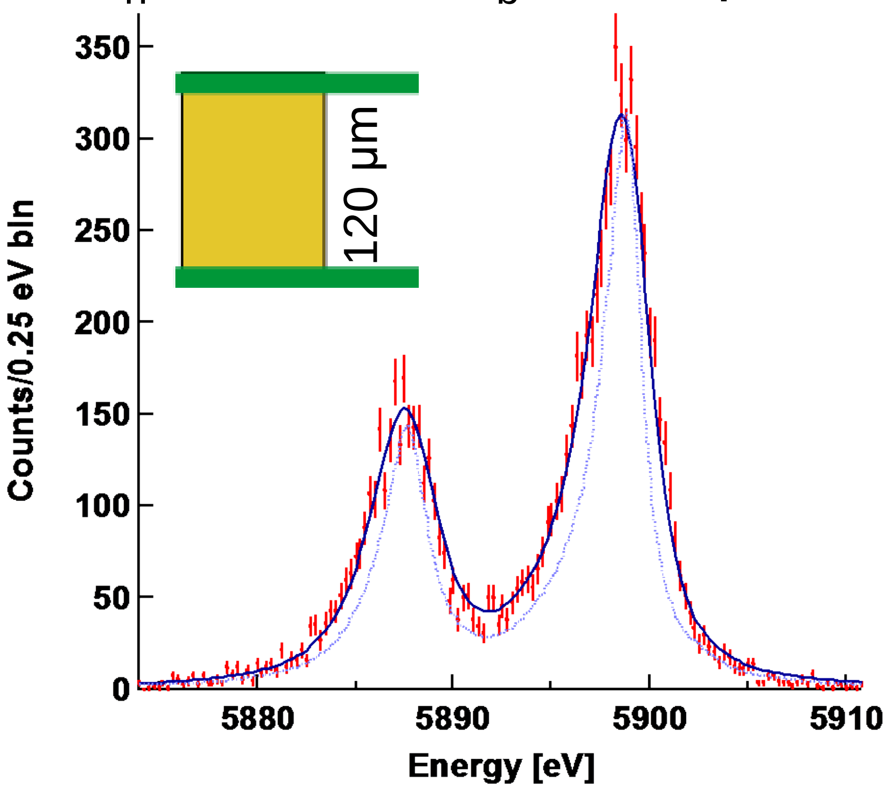

ΔE = 2.08 +/- 0.09 eV
Counts = 9,723

1:0.50

R_n = 82 mΩ, G_b = 79 pW/K

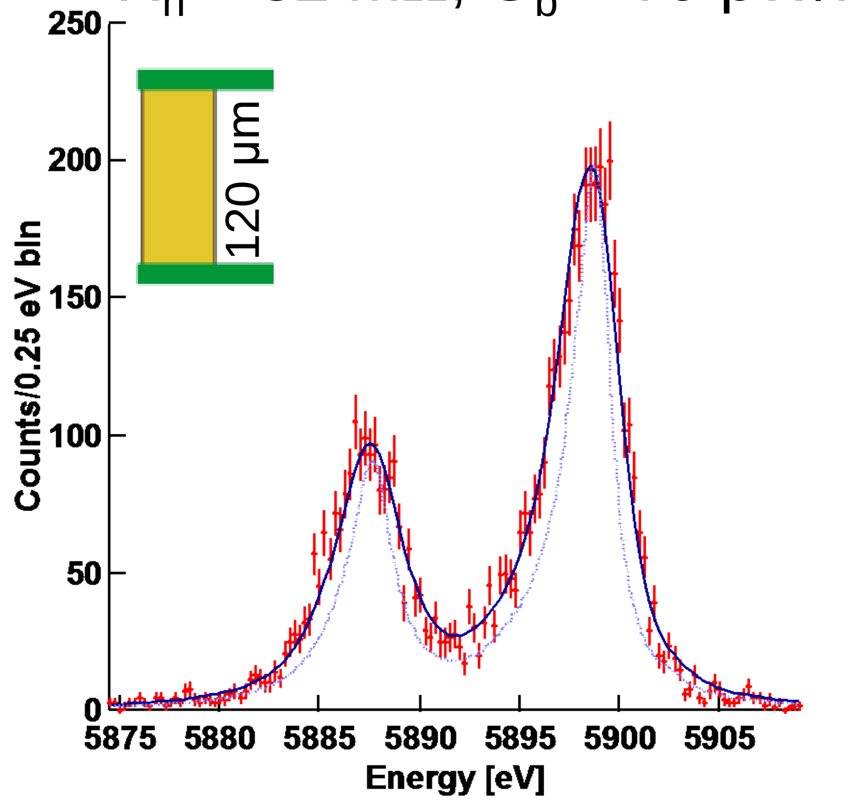

ΔE = 2.13 +/- 0.11 eV
Counts = 6,180

1:0.25

R_n = 160 mΩ, G_b = 65 pW/K

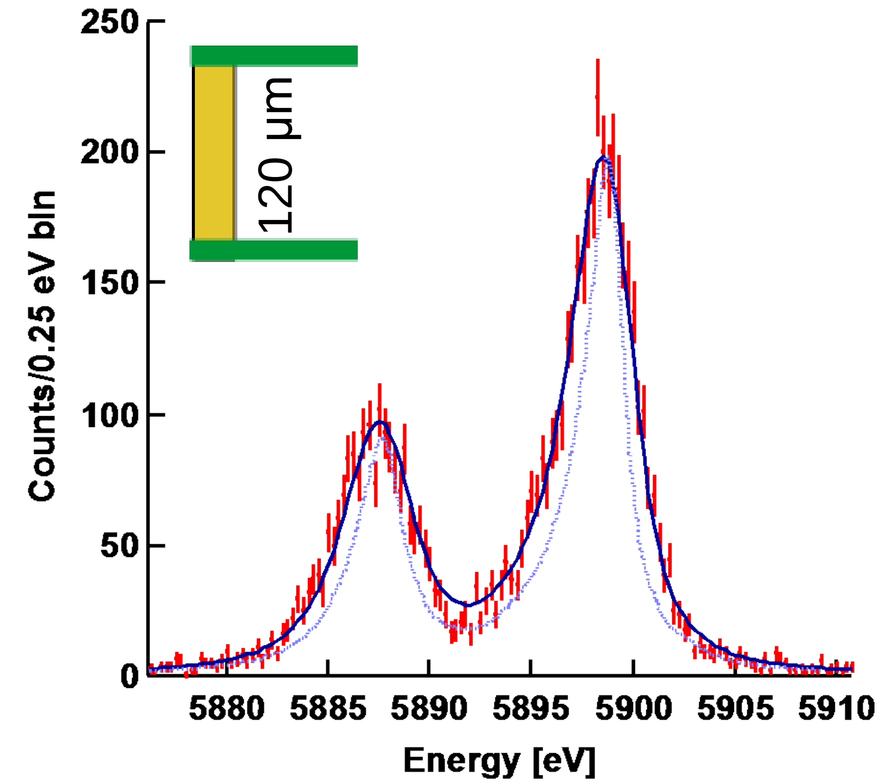

ΔE = 2.18 +/- 0.11 eV
Counts = 6,206

- First 120 μm high aspect ratio devices in DC testing.
- Preliminary measurements suggest no strong ΔE dependence on aspect ratio
- Added design flexibility: higher Z and lower $G_{b.}$
- First AC tests planned soon.

First large X-IFU array scale test parts yielded

- 90 mm diameter hexagonal chip and prototype detector array.
- 3540 sensors on 250 µm pitch.
- 960 pixels connected to bond pads.
- First DC tests planned for later this year.
- Later iteration will include coil-coupling for AC biased testing.

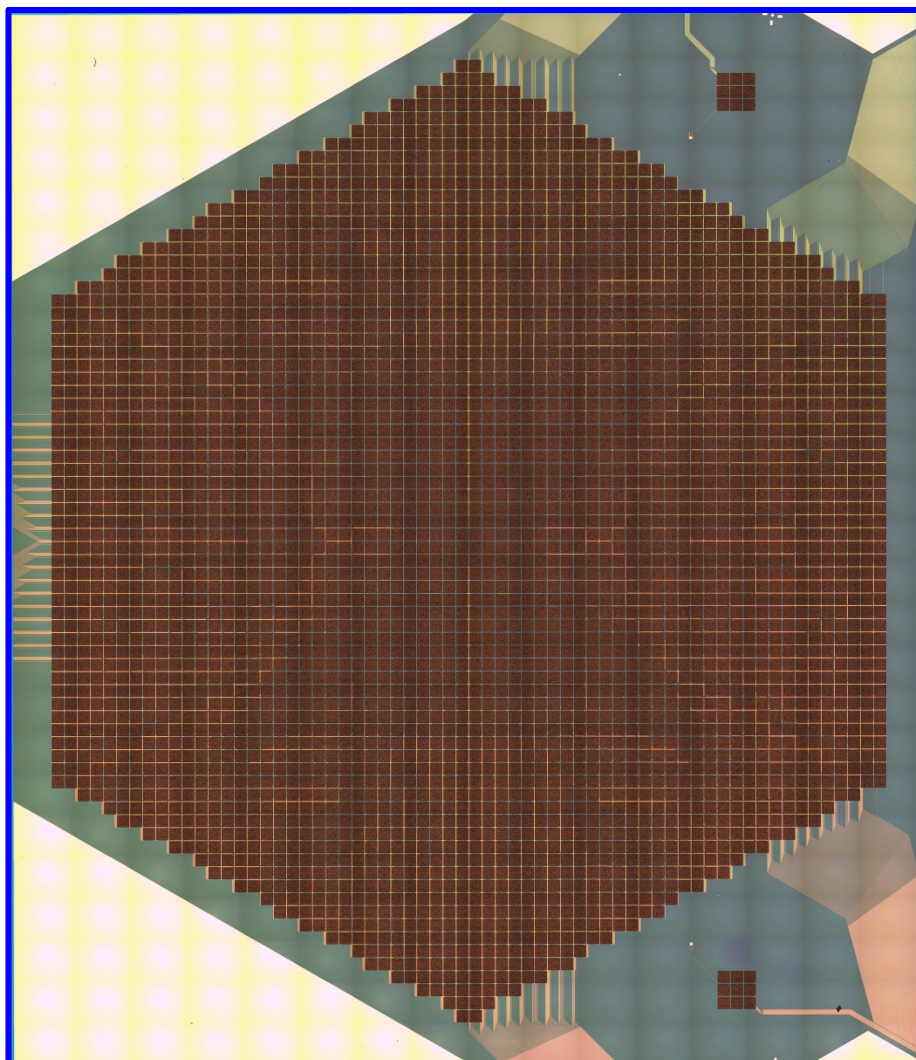

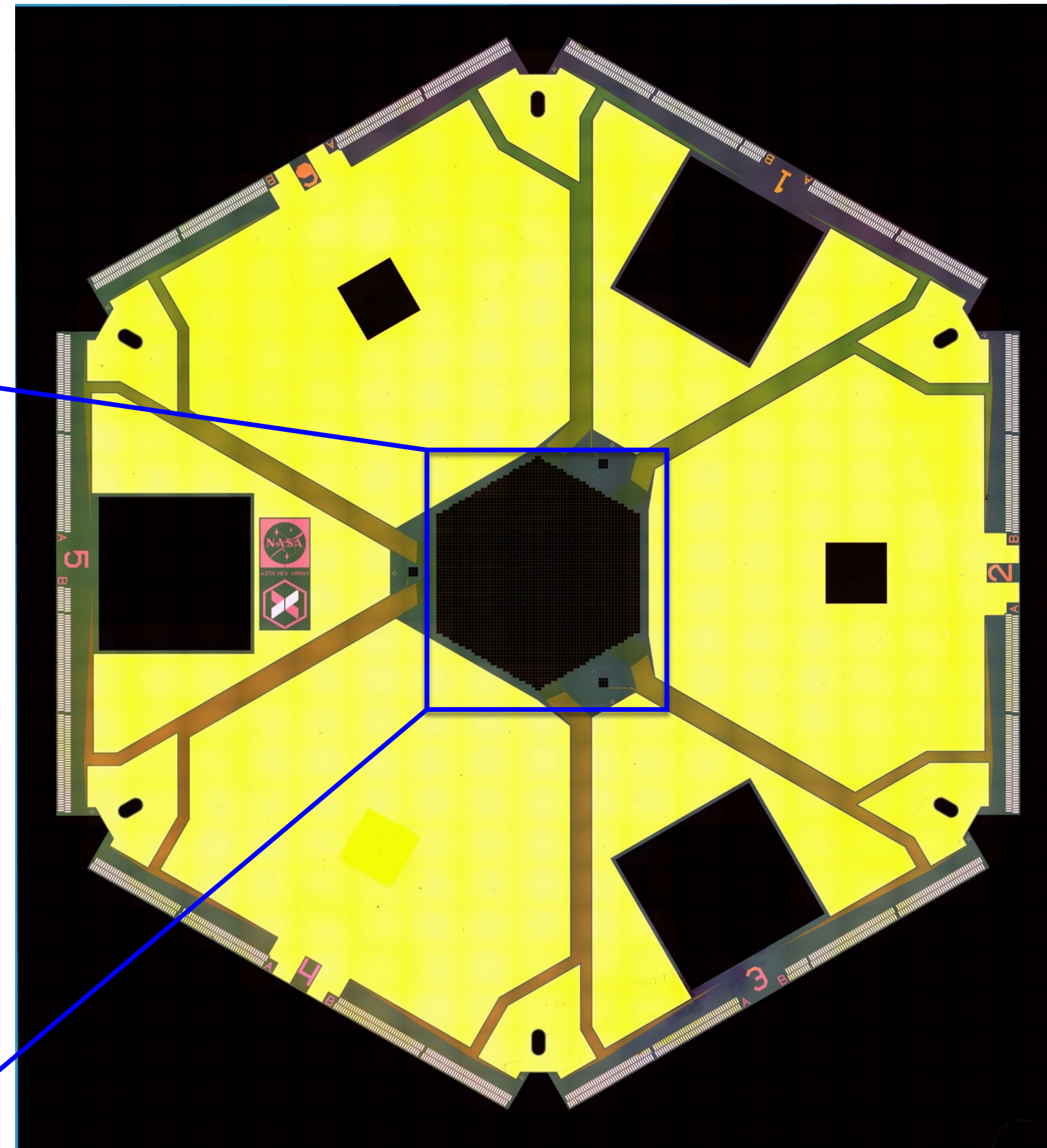

Summary

- Improved DC and AC pixel designs:
  - Evolved original 3-stripe 140 µm TES design to smaller TESs without stripes.
    - Larger transition phase-space without ‘kinks’ -> Improves array uniformity.
  - Developed first high-Z Mo/Au TESs for reduced AC Loss and + Josephson effect in AC TES.
    - Improved access good transition regions.
    - ***Break through energy resolution < 2.5 eV results for AC TESs at both low and high frequency.***
  - First high-Z uniform 32x32 arrays now delivered to SRON for 40-pixel FDM testing.

- Ongoing development activities:
  - First high aspect ratio devices in DC testing.
    - Designs offer addition parameter space for higher Z and low Gb.
    - AC testing planed for this fall.
  - First large scale X-IFU testing planned for 1000-pixel testing later this year.